Volume 1, No.1, March – April 2012
International Journal of Advanced Trends in Computer Science and Engineering
Available Online at www.warse.ijatcse.current

Recent Developments and Signal Processing of Low Driving Voltage and High Modulation Efficiency Electro-absorption Modulators (EAMs)

Ahmed Nabih Zaki Rashed
Electronics and Electrical Communications Engineering Department
Faculty of Electronic Engineering, Menouf 32951, Menoufia University, EGYPT
ahmed_733@yahoo.com

ABSTRACT

Electro-absorption (EA) modulators are very attractive devices for optical fiber communications because of their very low driving voltage, very high modulation efficiency and integratibility with lasers. However, conventional EA modulators are lumped electrode devices, whose speeds are limited by the total parasitics of the devices, which restricts the devices to very short length for high speed operation. This paper has presented the important transmission characteristics of EA modulators such as transmission performance efficiency, modulation photocurrent, insertion loss, extinction ratio, relative refractive index difference, and signal transmission quality, over wide range of the affecting parameters for different selected electro-absorption materials to be the major of interest.

Keywords: Low Driving Voltage, High Modulation Efficiency, Low Chirp, Reverse Bias Voltage, Speed Response

1. INTRODUCTION

The transmission bit rates in backbone telecommunication optical fibers are increasing rapidly, motivated by the explosive growth of Internet traffic. As the channel bit rate distance product increases, external modulation of the laser light is necessary to avoid the unacceptably high chirping of directly modulated lasers and to overcome the dispersion of standard single mode fiber [1]. $LiNbO_3$ electro-optic modulators are currently widely used in low bit-rate applications. However, the high drive voltage requirement for these modulators becomes a big problem at high bit rates. On the other hand, Electro-Absorption (EA) modulators based on quantum confined Stark effect in Multiple Quantum Wells (MQWs) are advantageous for their high speed, low drive voltage, high extinction ratio and integratibility with lasers. Currently, EA modulators use lumped electrode structures, which limit the device bandwidth by the RC time constant and require a short device length for high speed operation [2].

Nonlinear optical and linear electro-optic materials find use in switching and modulation devices for photonic integrated circuits. For modulators in telecommunications small size and modulation voltages are desired. Both Electro-Absorption (EA) and Electro-Optic (EO) modulators are candidates for use in external modulation links in telecommunications. These modulators can be realized using either bulk semiconductor materials [3] or materials with multiple quantum dots or wells. Electro-absorption modulators have been widely used in fiber optic communication systems for their small size, low driving voltage, low chirp, and high bandwidth [4]. In addition, due to matching of material systems, EAMs can be easily integrated with other optical components, such as semiconductor lasers, semiconductor optical amplifiers, and attenuators. Since many material properties, such as bandgap, refractive index, and thermal conductivity, change with temperature, internal heating must be considered in the design of an Electro-Absorption Modulator (EAM). This is especially important for high power operation, because large heating can damage the device. The input power tolerance of InGaAsP EAMs have been investigated experimentally in terms of breakdown phenomena, and it was shown that optical power for breakdown depended on bias voltage and operating wavelength [5]. In addition, since incident light is attenuated along the modulator, the temperature distribution is not uniform, as measured by [6], using a liquid crystal technique. The positive feedback from the interaction of absorption and temperature may make light absorption and heating greatly localized at the input of the modulator, and the peak temperature increased nonlinearly with incident light power and bias voltage.

EAMs are among the most important components of high speed Wavelength Division Multiplexing (WDM) optical communications devices and systems. EAMs are widely used as stand alone devices, as part of electro-absorption modulated lasers, and as part of multi-component planar lightwave circuits. Since the first proposed EAMs based on optical absorption of light in a bulk structure more than two decades ago [7], advances have been made in modulator performances such as extinction ratio, polarization insensitivity, and bandwidth. MQWs structures in the active region have become the structures of choice for EAMs due to their improved extinction and reduced polarization sensitivity through applied strain [8]. While lumped electrode devices have demonstrated performance at rates of 10 Gb/s and higher, the more recent traveling wave electrode devices have been shown to work at rates of 43 Gb/s and above [9]. Compared to the other popular class of modulators, Mach Zehnder based Lithium Niobate modulators, EAMs offer a number of advantages such as low voltage drive, small size, high bandwidth, and potential for monolithic integration with other optoelectronic devices.

For good performance of the modulator, a high extinction ratio is necessary.

In the present study, EAMs are typically electrically driven to vary the electric field across the device and hence the optical transmission through it. Waveguide EAMs are increasingly being used in optical networks since they can be monolithically integrated with continuous wave edge emitting laser diodes to create low cost, high speed optical transmitters. The high speed transmission characteristics of electro-absorption modulators under wide range of the affecting parameters are investigated. The maximum modulation bandwidth is deeply analyzed. The theoretical modulation response of the EAM is derived from the standard rate equations, and the qualitative form is in agreement with the measured results.

2. THEORETICAL MODEL ANALYSIS

The investigation of both the thermal and spectral variations of the electroptic (EO) modulator effective refractive index (n_e) require Sellmeier equation. The set of parameters required to completely characterize the temperature dependence of the refractive-index is given below, Sellmeier equation is under the form [10][11]:

$$n_e = \sqrt{1 + \frac{A_1\lambda^2}{\lambda^2 - A_2^2} + \frac{A_4\lambda^2}{\lambda^2 - A_4^2} + \frac{A_5\lambda^2}{\lambda^2 - A_6^2}} \quad , \qquad (1)$$

For different selected semiconductor electro-optic materials based EOMs, where the Sellemeier coefficients for Silicon (Si), Germanium (Ge), and arsenic trisulfide (AS_2S_3) are listed in the following Table 1.

Table 1: Sellemeier coefficients for different selected semiconductor EO materials [12][13][14][15]

Coefficients	Si	Ge	AS_2S_3
A_1	10.6684293 (T/T_0)	14.7587446 (T/T_0)	4.07205767 (T/T_0)
A_2	0.301516485 $(T/T_0)^2$	0.434303403 $(T/T_0)^2$	0.208841706 $(T/T_0)^2$
A_3	0.0030434748 (T/T_0)	0.235256294 (T/T_0)	0.744196974 (T/T_0)
A_4	1.13475115 $(T/T_0)^2$	1.26245893 $(T/T_0)^2$	0.3959647 $(T/T_0)^2$
A_5	1.54133408 (T/T_0)	-24.8822748 (T/T_0)	0.988377784 (T/T_0)
A_6	1104 $(T/T_0)^2$	1302 $(T/T_0)^2$	27.7481958 $(T/T_0)^2$

Where T is the ambient temperature, and T_0 is the room temperature respectively. Then the first and second differentiation of empirical equation with respect to operating wavelength λ yields the following expressions:

$$\frac{dn_e}{d\lambda} = \frac{-1}{n_e}\left(\frac{A_1A_2^2\lambda}{\left(\lambda^2 - A_2^2\right)^2} + \frac{A_3A_4^2\lambda}{\left(\lambda^2 - A_4^2\right)^2} + \frac{A_5A_6^2\lambda}{\left(\lambda^2 - A_6^2\right)^2}\right), \qquad (2)$$

$$\frac{d^2n_e}{d\lambda^2} = \frac{1}{n_e}\left(\frac{A_1A_2^2\left(3\lambda^2 + A_2^2\right)}{\left(\lambda^2 - A_2^2\right)^3} + \frac{A_3A_4^2\left(3\lambda^2 + A_4^2\right)}{\left(\lambda^2 - A_4^2\right)^3} + \frac{A_5A_6^2\left(3\lambda^2 - A_6^2\right)}{\left(\lambda^2 - A_6^2\right)^3} - \left(\frac{dn_e}{d\lambda}\right)^2\right), \qquad (3)$$

The change in mode effective index varies linearly with the applied voltage, and the change in the mode effective index due to applied voltage (Δn (V)) is given in below [16][17]:

$$\Delta n_e(V) = \frac{0.5 r_{41} n_e^3 \Gamma V}{t} \quad , \qquad (4)$$

Where r_{41} is the electro-optic coefficient, t is the thickness of the modulator thickness, Γ is the confinement factor, and V is the applied bias voltage. Given the material absorption coefficient α and optical confinement of the intrinsic layer, and assuming unity quantum efficiency, the modulation photocurrent I_{mod} can be calculated for length L of modulator:

$$I_{\mathrm{mod}} = \frac{P q \lambda \left(1 - \exp\left(-\alpha \Gamma L\right)\right)}{2\pi c h}, \qquad (5)$$

Where c is the speed of light, h is the Planck's constant, P is the input light power, q is the electron charge, and λ is the operating optical signal wavelength. As well as the material absorption coefficient, α in μm^{-1}, which can be expressed as a function of operating optical signal wavelength by using MATLAB fitting program for different semiconductor materials based EOMs as [18][19]:

$\alpha = 0.7721 + 0.005868\,\lambda - 0.0931\,\lambda^2$, (Si) (6)

$\alpha = 44.5643 - 0.008893\,\lambda + 0.00135\,\lambda^2$, (Ge) (7)

$\alpha = 0.2345 + 0.005143\,\lambda - 0.0852\,\lambda^2$, (AS_2S_3) (8)

The transmission spectra, T_m, insertion loss, IL, and extinction ratio, ER, of the different EA modulator devices with using MATLAB curve fitting program as [20][21][22]:

$$T_m = 0.854 - 0.00297\alpha V^{-1} + 0.0765\alpha^2 V^{-2} - 0.0037\alpha^3 V^{-3} \qquad (9)$$

$$IR = 35.54 - 0.008\alpha + 0.00076\alpha^2 - 0.03\alpha^3, \text{ dB} \qquad (10)$$

$$ER = 9.76 + 0.765\alpha V - 0.00043\alpha^2 V^2 + 0.054\alpha^3 V^3, \text{ dB} \qquad (11)$$

3. SIMULATION RESULTS AND PERFORMANCE ANALYSIS

The recent developments of low driving voltage and high modulation efficiency of EAMs over wide range of the affecting operating parameters have been deeply investigated as shown in Table 2.

Table 2: Proposed operating parameters for electro-absorption modulators

Parameter	Definition	Value and unit
$T=T_0$	Ambient temperature=room temperature	300 K
L	Modulator length	300 μm
t	Modulator thickness	25 μm
P	Input light power	0.1 Watt—0.5 Watt
λ	Operating signal wavelength	1.3 μm—1.55 μm
r_{41}	Electoptic coefficient for AS_2S_3	35 Pm/volt
	Electoptic coefficient for Ge	48 Pm/volt
	Electoptic coefficient for Si	23 Pm/volt
Γ	Confinement factor	0.9

V	Applied bias voltage	1Volt—10 Volt
q	Electron charge	$1.6x10^{-19}C$
c	Speed of light	$3x10^{8}$ m/sec
h	Planck's constant	$6.02x10^{-34}J.sec$

Based on the model equations analysis, assumed set of the operating parameters, and the set of the series of the Figs. (1-11), the following facts are assured:

i) Figs. (1, 2) have assured that effective relative refractive index difference increases with increasing applied bias voltage and decreasing operating optical signal wavelength for different materials under study. We have observed that the Ge material has presented the highest effective relative refractive index difference compared to other materials.

ii) As shown in Figs. (3, 4) have proved that modulation photo current increases with increasing both input light power and operating optical signal wavelength for different materials under considerations. We have indicated that the As_2S_3 material has presented the highest modulation photo current compared to other materials.

iii) Figs. (5-7) have demonstrated that modulator transmission increases with increasing operating optical signal wavelength and decreasing applied bias voltage for different materials under study. We have also observed that the As_2S_3 material has presented the highest modulator transmission compared to other materials.

iv) Fig. 8 has indicated that modulator insertion loss decreases with increasing operating optical signal wavelength for different materials under considerations. As well as we have indicated that the As_2S_3 material has presented the lowest insertion loss compared to other materials.

v) Figs. (9-11) have assured that modulator extinction ratio increases with increasing both operating optical signal wavelength and applied bias voltage for different materials under study. Moreover we have also observed that the As_2S_3 material has presented the highest extinction ratio compared to other materials.

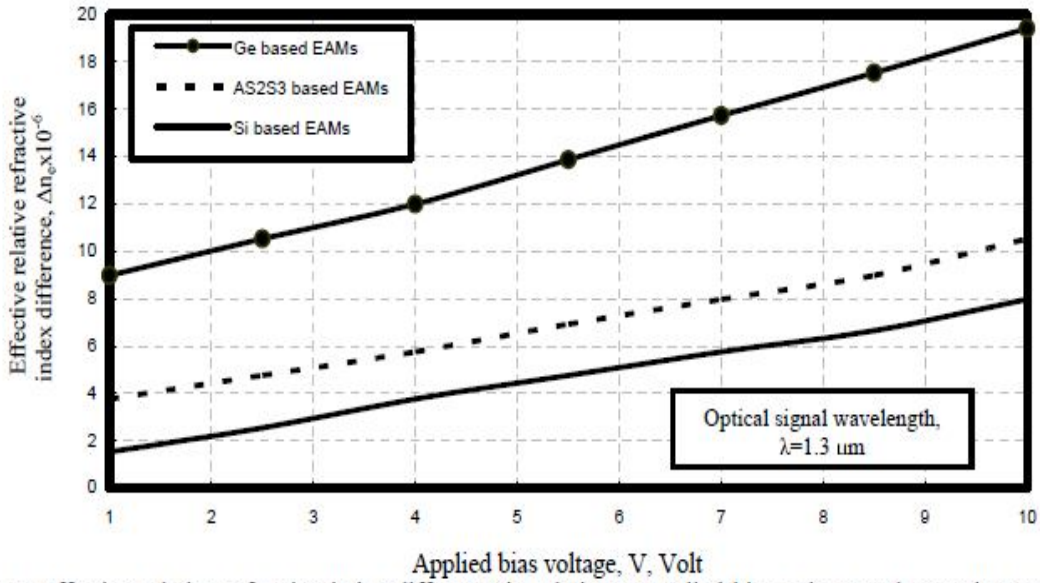

Fig. 1. Effective relative refractive index difference in relation to applied bias voltage and operating optical signal wavelength at the assumed set of the operating parameters.

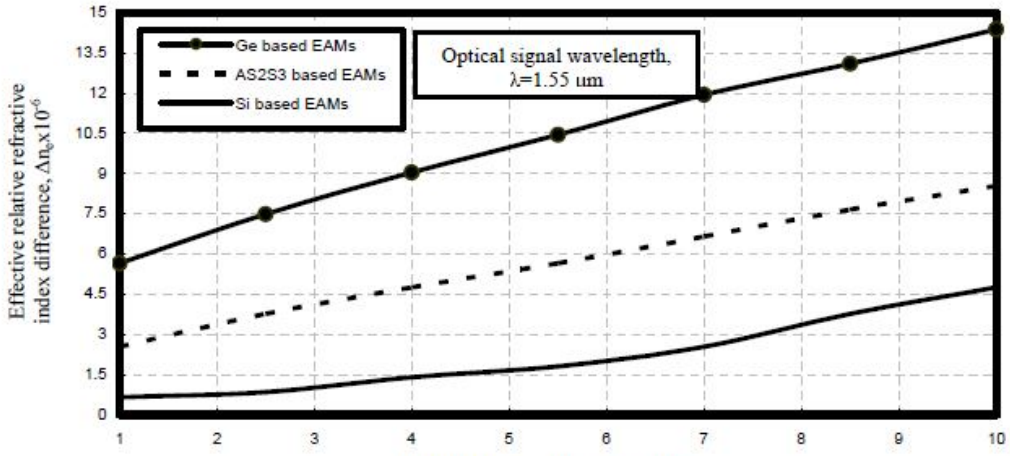

Fig. 2. Effective relative refractive index difference in relation to applied bias voltage and operating optical signal wavelength at the assumed set of the operating parameters.

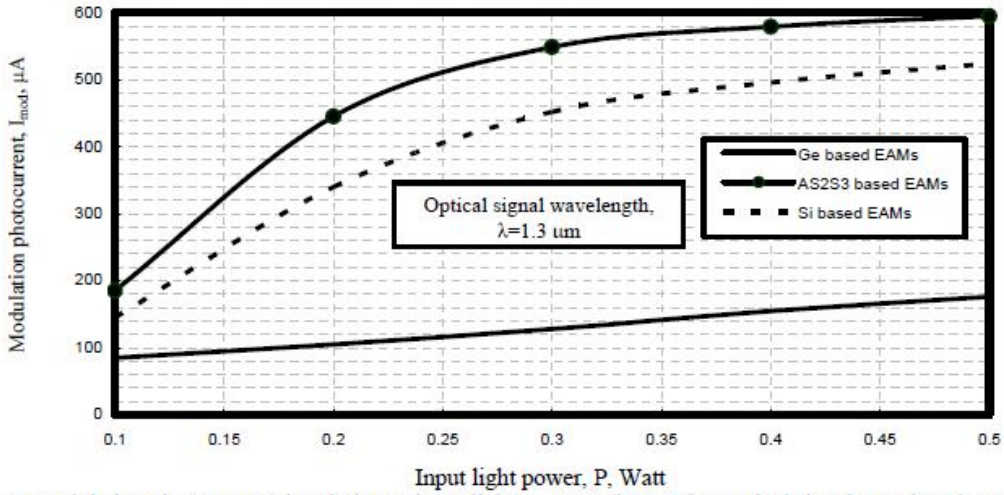

Fig. 3. Modulation photo current in relation to input light power and operating optical signal wavelength at the assumed set of the operating parameters.

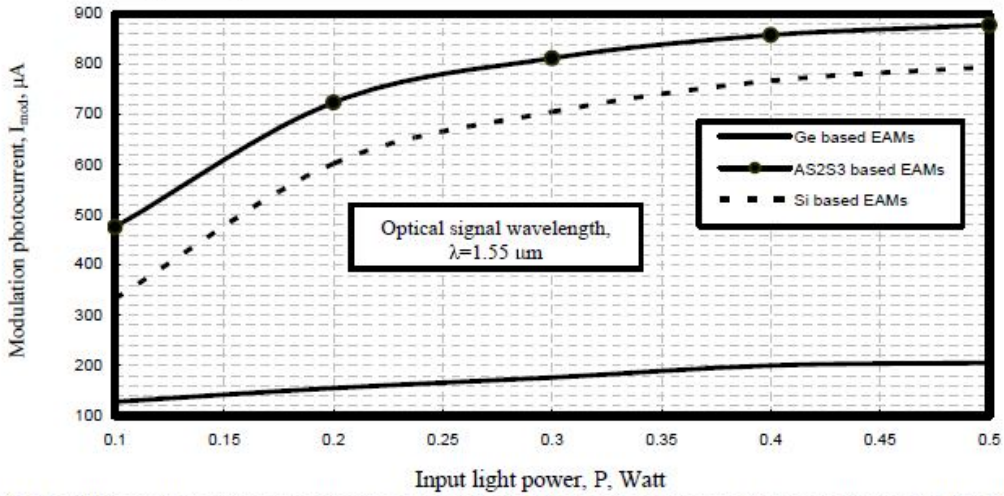

Fig. 4. Modulation photo current in relation to input light power and operating optical signal wavelength at the assumed set of the operating parameters.

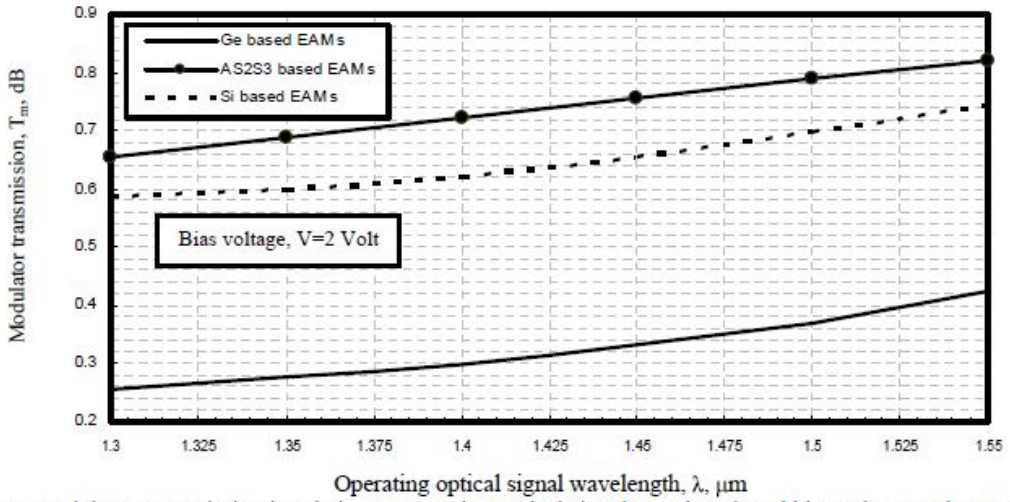

Fig. 5. Modulator transmission in relation to operating optical signal wavelength and bias voltage at the assumed set of the operating parameters.

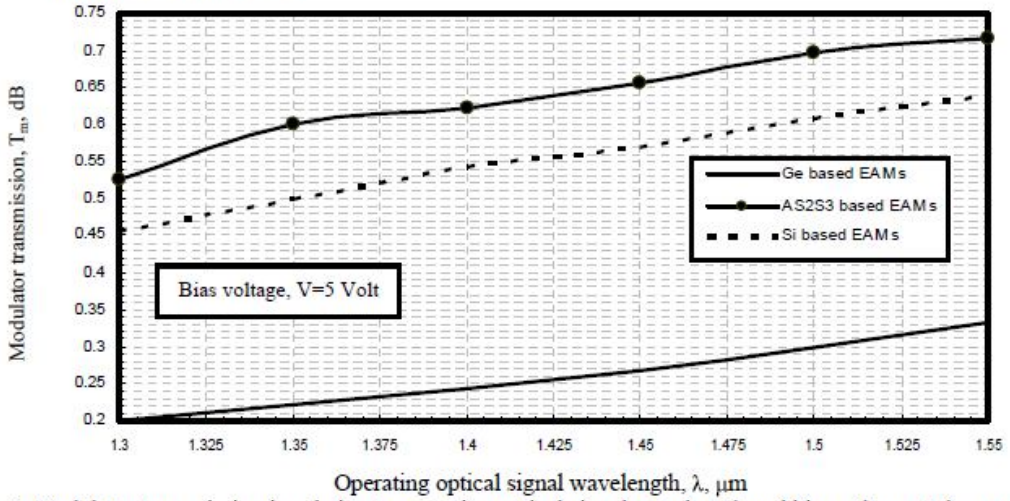

Fig. 6. Modulator transmission in relation to operating optical signal wavelength and bias voltage at the assumed set of the operating parameters.

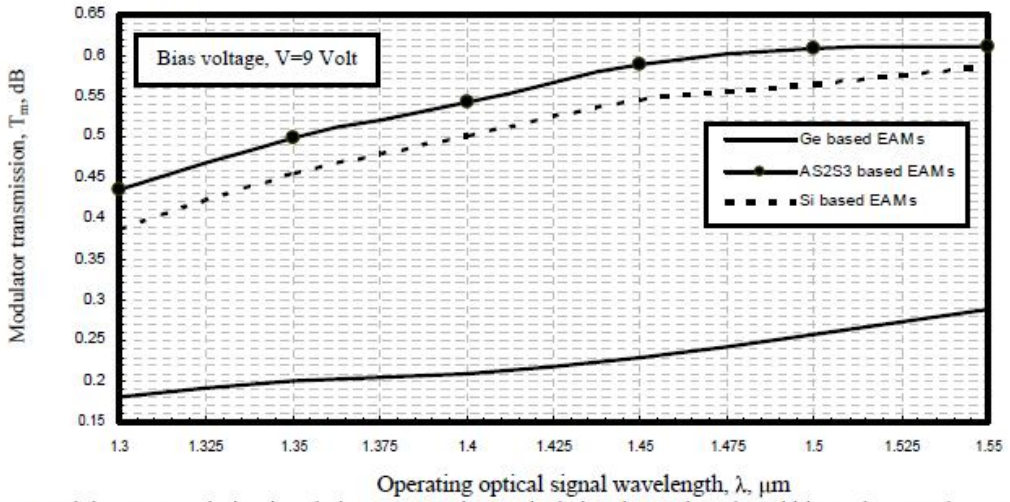

Fig. 7. Modulator transmission in relation to operating optical signal wavelength and bias voltage at the assumed set of the operating parameters.

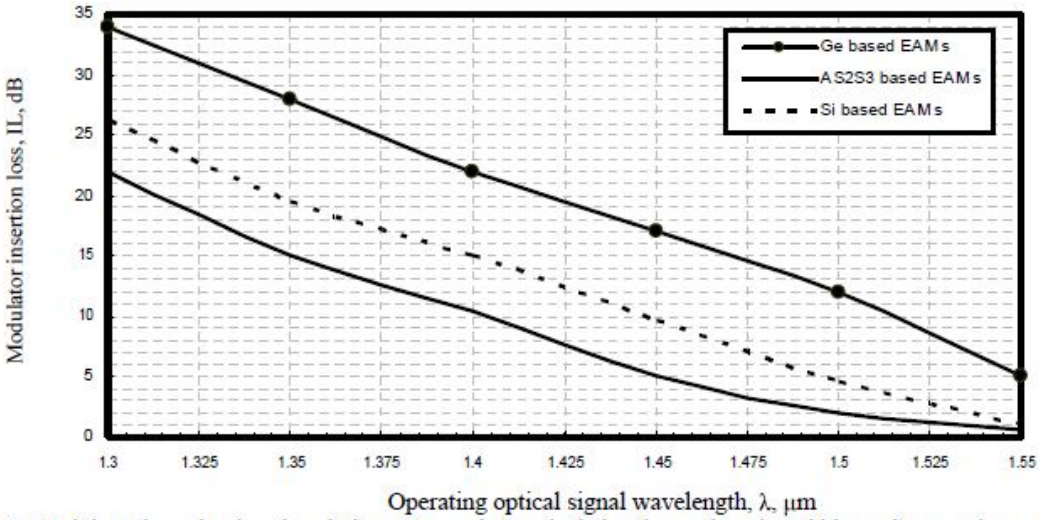

Fig. 8. Modulator insertion loss in relation to operating optical signal wavelength and bias voltage at the assumed set of the operating parameters.

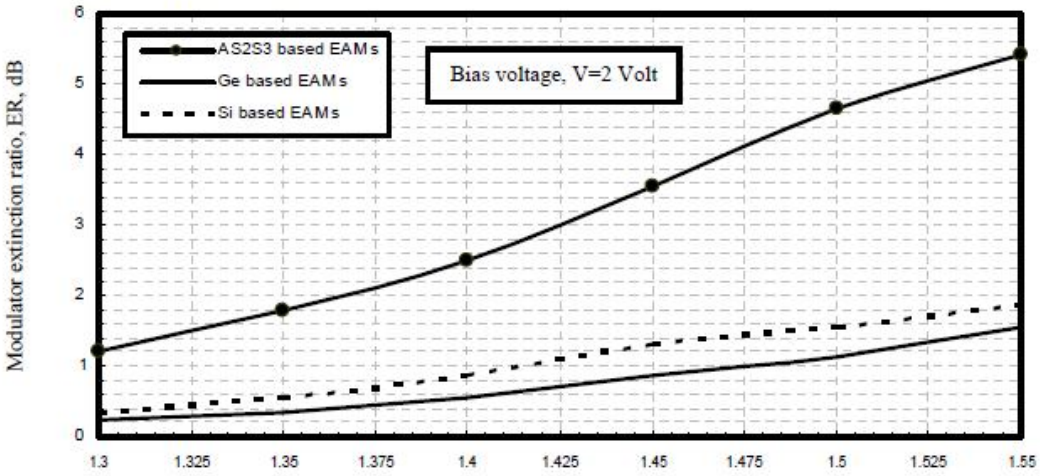

Fig. 9. Modulator extinction ratio in relation to operating optical signal wavelength and bias voltage at the assumed set of the operating parameters.

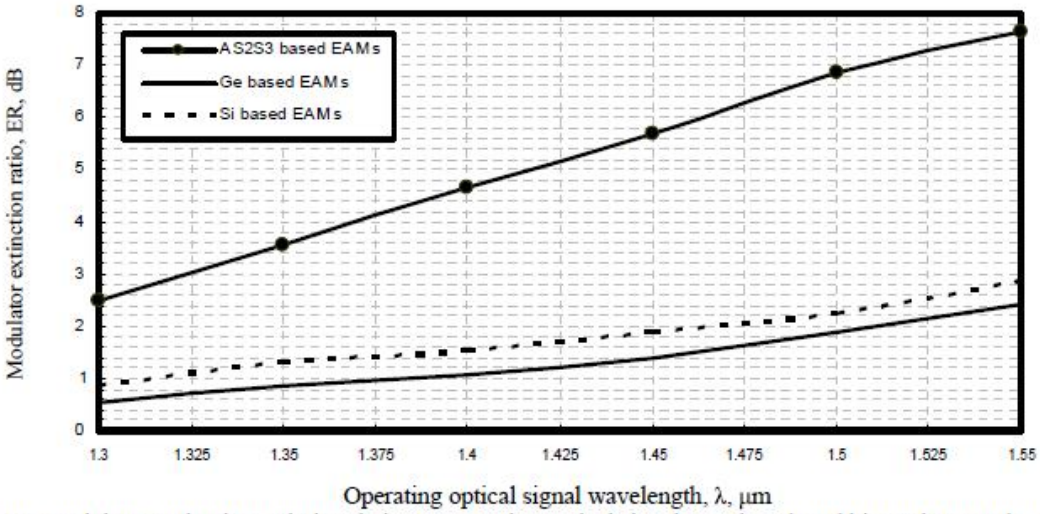

Fig. 10. Modulator extinction ratio in relation to operating optical signal wavelength and bias voltage at the assumed set of the operating parameters.

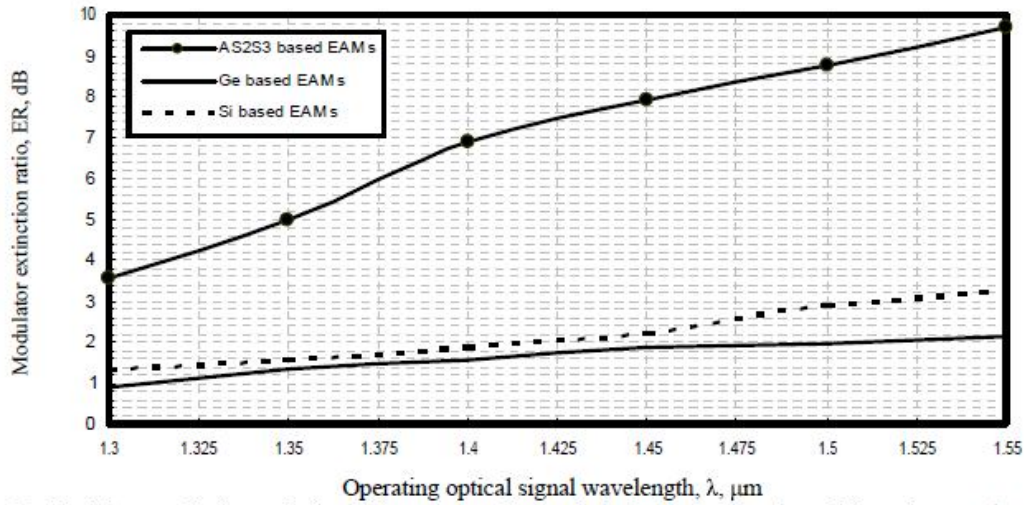

Fig. 11. Modulator extinction ratio in relation to operating optical signal wavelength and bias voltage at the assumed set of the operating parameters.

4. CONCLUSION

Traveling wave electro absorption modulators using the Si, Ge, and AS_2S_3 material system have been demonstrated. For a 300 μm long device, a extinction ratio with arrange of 2-10 dB, insertion loss with the range of 5-30 dB, and modulator transmission with the range of 0.2-0.9 dB are achieved for the selected materials based EAMs under considerations. It is indicated that As_2S_3 has presented the highest modulation photo current, transmission, and the extinction ratio, and the lowest insertion loss compared to other materials under study and under the same operating conditions. These results show that with good design, electro-absorption modulators can overcome the insertion loss limitation and obtain higher speed, lower driving voltage and larger extinction ratio for optical fiber communication applications with using As_2S_3 based EAMs.

REFERENCES

1. Min Chen, Liang Zhou, Takahiro Hara, Yang Xiao and Victor C.M. Leung. **Advances in Multimedia Communications**, International Journal of Communication Systems, Vol. 24, No. 10, pp. 1243-1245, 2011.

2. Abd El-Naser A. Mohammed, Ahmed Nabih Zaki Rashed, and Mohammed S. F. Tabour. **Transmission Characteristics of Radio over Fiber (ROF) Millimeter Wave Systems in Local Area Optical Communication Networks**, International Journal of Advanced Networks and Applications, Vol. 2, No. 6, pp. 876-886, 2011.

3. Maksymiuk, and J. Siuzdak. **Modeling of Low Frequency Modal Noise Induced by Multimode Couplers in Cascade Connections**, Optica Applicata, Vol. 41, No. 3, pp. 649-660, 2011.

4. Abd El–Naser A. Mohamed, Ahmed Nabih Zaki Rashed, Sakr A. S. Hanafy, and Amira I. M. Bendary. **Electro optic Polymer Modulators Performance Improvement With Pulse Code Modulation Scheme in Modern Optical Communication Networks**, International Journal of Computer Science and Telecommunications (IJCST), Vol. 2, No. 6, pp. 30-39, Sep. 2011.

5. Q. TAO, F. Luo, Q. Liang, Z. Wan, X. Song, and X. Liu. **Optical Switch Based on Cascaded SOI Nonlinear Directional Coupler**, Optica Applicata, Vol. 41, No. 3, pp. 669-678, 2011.

6. Abd El-Naser A. Mohammed, Mohamed M. E. El-Halawany, Ahmed Nabih Zaki Rashed, and Sakr Hanafy. **High Performance of Plastic Optical Fibers within Conventional Amplification Technique in Advanced Local Area Optical Communication Networks**, International Journal of Multidisciplinary Sciences and Engineering (IJMSE), Vol. 2, No. 2, pp. 34-42, 2011.

7. T. Kawanishi, T. Sakamoto, and M. Izutsu. **High Speed Control of Lightwave Amplitude, Phase, and Frequency by use of Electrooptic Effect**, IEEE Journal of Selected Topics in Quantum Electronics, Vol. 13, No. 1, pp. 79–91, 2007.

8. H. V. Pham, H. Murata, and Y. Okamura. **Travelling Wave Electro optic Modulators With Arbitrary Frequency Response Utilising Non Periodic Polarization Reversal**, Electronics Letters, Vol. 43, No. 24, pp. 1379–1381, 2007.

9. Abd El-Naser A. Mohammed, Mohamed Metwae'e, Ahmed Nabih Zaki Rashed, and Amira I. M. Bendary. **Recent Progress of LiNbO3 Based Electrooptic Modulators with Non Return to Zero (NRZ) Coding in High Speed Photonic Networks**, International Journal of Multidisciplinary Sciences and Engineering (IJMSE), Vol. 2, No. 4, pp. 13-21, July 2011.

10. Ahmed Nabih Zaki Rashed. **New Trends of Forward Fiber Raman Amplification for Dense Wavelength Division Multiplexing (DWDM) Photonic Communication Networks**, International Journal on Technical and Physical Problems of Engineering (IJTPE), Vol. 3, No. 2, pp. 30-39, June 2011.

11. Abd El-Naser A. Mohammed, Mohamed M. E. El-Halawany, Ahmed Nabih Zaki Rashed, and Mohammed S. F. Tabour. **High Transmission Performance of Radio over Fiber Systems over Traditional Optical Fiber Communication Systems Using Different Coding Formats for Long Haul Applications**, International Journal of Advances in Engineering & Technology (IJAET), Vol. 1, No. 3, pp. 180-196, July 2011.

12. M. Ghanbarisabagh, M. Y. Alias and H. A. Abdul-Rashid. **Cyclic Prefix Reduction for 20.48 Gb/s Direct Detection Optical OFDM Transmission over 2560 km of SSMF**, International Journal of Communication Systems, Vol. 24, No. 11, pp. 1407-1417, 2011.

13. Kozanecka , D. Szmigifel, K. Switkowski, E. Schabbalcerzak and M. Siwy. **Electro Optic Activity of an Azopolymer Achieved Via Poling With the Aid of Silicon Nitride Insulating Layer**, Optica Applicata, Vol. 41, No. 3, pp. 777-785, 2011.

14. Abd El-Naser A. Mohammed, M. Metawe'e, Abd El-Fattah Saad and Mohammed Tabbour. **Recent Applications of the Electrooptic Modulators in Radio Over Fiber (ROF)**, Journal of Media and Communication Studies, Vol. 1, No. 6, pp. 106-115, 2009.

15. V. Krishnamoorthy, R. Ho, X. Zheng, H. Schwetman, J. Lexau, P. Koka, G. Li, I. Shubin, and J. E. Cunningham. **Computer Systems Based on Silicon Photonic Interconnects**, Proc. IEEE, Vol. 97, No. 7, pp. 1337–1361, 2009.

16. Abd El Naser A. Mohammed, Ahmed Nabih Zaki Rashed, Gaber E. S. M. El-Abyad, and Abd-El-fattah A. Saad. **Applications of Conventional and A thermal Arrayed Waveguide Grating (AWG) Module in Active and Passive Optical Networks (PONs)**, International Journal of Computer Theory and Engineering (IJCTE), Vol. 1, No. 3, pp. 290-298, 2009.

17. W. Fang, H. Park, O. Cohen, R. Jones, M. J. Paniccia, and J. E. Bowers. **Electrically Pumped Hybrid AlGaInAs Silicon Evanescent Laser**, Opt. Express, Vol. 14, No. 20, pp. 9203–9210, 2006.

18. J. Liu, X. Sun, R. Camacho-Aguilera, L. C. Kimerling, and J. Michel. **Ge on Si Laser Operating at Room Temperature**, Opt. Lett., Vol. 35, No. 5, pp. 679–681, 2010.

19. D. Ahn, C. Y. Hong, J. Liu, W. Giziewicz, M. Beals, L. C. Kimerling, J. Michel, J. Chen, and F. X. Kärtner. **High Performance Waveguide Integrated Ge Photodetectors**, Opt. Express, Vol. 15, No. 7, pp. 3916–3921, 2007.

20. L. Vivien, M. Rouvière, J. M. Fédéli, D. Marris-Morini, J. F. Damlencourt, J. Mangeney, P. Crozat, L. El Melhaoui, E. Cassan, X. Le Roux, D. Pascal, and S. Laval. **High Speed and High Responsivity Germanium Photodetector Integrated in A Silicon On Insulator Microwaveguide**, Opt. Express, Vol. 15, No. 15, pp. 9843–9848, 2007.

21. D. Feng, S. Liao, P. Dong, N.-N. Feng, H. Liang, D. Zheng, C.-C. Kung, J. Fong, R. Shafiiha, J. Cunningham, A. V. Krishnamoorthy, and M. Asghari. **High Speed Ge Photodetector Monolithically Integrated With Large Cross Section Silicon On Insulator Waveguide**, Appl. Phys. Lett., Vol. 95, No. 26, pp. 261-263, 2009.

22. N. Feng, P. Dong, D. Zheng, S. Liao, H. Liang, R. Shafiiha, D. Feng, G. Li, J. Cunningham, A. Krishnamoorthy, and M. Asghari. Vertical p-i-n Germanium Photodetector With High External Responsivity Integrated With Large Core Si Waveguides, Opt. Express, Vol. 18, No. 1, pp. 96–101, 2010.

